

Distributed surveillance by a swarm of UAVs operating under positional uncertainty

Nikolaos Bousias
Dept. of Electrical and
Computer Engineering
University of Patras
Rio 26500, Greece
up1020031@upnet.gr

Sotiris Papatheodorou
Dept. of Computing
Imperial College London
London SW7 2AZ, UK
sotirisp@protonmail.com

Mariliza Tzes
Dept. of Electrical and Systems
Engineering (GRASP Lab)
University of Pennsylvania
Philadelphia, PA 19104, U.S.A.
mariliza.tze@gmail.com

Anthony Tzes
Dept. of Electrical and
Computer Engineering
NYU AD
Abu Dhabi 129188, U.A.E.
anthony.tzes@nyu.edu

Abstract—This article proposes a collaborative control framework for an autonomous aerial swarm tasked with the surveillance of a convex region of interest. Each Mobile Aerial Agent (MAA) is equipped with a Pan-Tilt-Zoom (PTZ) camera of conical FOV and suffers from sensor-induced positional uncertainty. By utilizing a Voronoi-free tessellation strategy and a gradient scheme, the heterogeneous swarm self-organizes in a distributed manner to monotonically achieve optimal collective visual coverage of the region of interest, both in terms of quality and total area. Simulation studies are offered to investigate the effectiveness of the suggested scheme.

Index Terms—Cooperating Robots, Swarms, Multi-Robot Systems, Area Coverage

I. INTRODUCTION

Mobile robot teams have several potential applications, one of the frequently studied ones being area coverage problems. Coverage problems can be broadly categorized as static or sweep coverage. In static or blanket coverage [1], [2] the objective of the mobile agents is a static configuration at which some performance criterion is optimized. In dynamic or sweep coverage problems [3], [4] the performance criterion is time-varying, resulting in the agents moving constantly. Other ways to categorize coverage problems are based on the properties of the region of interest [5], [6], of the dynamic model of the mobile agents [7], [8] or on the type of their onboard sensors [9], [10]. The most common approach to coverage problems is geometric optimization [11] with other proposed approaches being event-triggered control [12], game theory [13], annealing algorithms [14] and model predictive control [15].

An inherent characteristic of most positioning systems is the uncertainty in their measurements. Some proposed solutions applied to mobile robots are probabilistic methods [16], safe trajectory planning [17] or the use of Voronoi-like partitioning schemes [18], [19]. In this article the positioning uncertainty model is similar to the one used in [18], [19] but the approach followed differs. Instead of employing a Voronoi-like space partitioning, the positioning uncertainty is incorporated in the agents' sensing patterns and the sensed space is partitioned using a Voronoi-free technique similar to [20].

Aerial agents are a popular platform for area coverage tasks due to their high mobility and versatility. The case of cameras with up to 3 translational and 3 rotational degrees of freedom

has been examined in [21] and an algorithm for information exchange has also been developed. In this work however the cameras are not allowed to zoom and the cameras' localization is precise. Moreover, regions covered by multiple agents contribute more to the objective, thus favoring overlapping between the agents' sensed regions. Previous works have examined downwards facing cameras [20], [22] and although positioning uncertainty has been successfully incorporated in these control schemes [19], it was done using a Voronoi-like partitioning which is not easy to generalize in the case of pan-tilt-zoom cameras. Pan-tilt-zoom camera networks have been examined using Voronoi-like diagrams in [23] although in that work the cameras were stationary instead of being affixed on mobile agents. In the present work the MAAs have 3 translational degrees of freedom and are equipped with pan-tilt-zoom cameras. The MAAs' planar positioning uncertainty is taken into account by using a Voronoi-free partitioning scheme. Additionally, regions sensed by multiple agents do not contribute more to the objective, thus favoring separation of the MAAs' sensing patterns. It should be noted that what the best approach concerning the overlapping of sensing patterns depends entirely on the intended use-case and the one used in this article can not be considered strictly better or worse than the one used in [21].

II. PROBLEM STATEMENT

We assume a compact convex region $\Omega \in \mathbb{R}^2$ to be placed under surveillance by a swarm of n MAAs, each positioned at $X_i = [x_i, y_i, z_i]^T, i \in I_n$ where $I_n = \{1, \dots, n\}$. We define the vector $q_i = [x_i, y_i]^T \in \Omega$ denoting the projection of each MAA on the plane. Each MAA can fly within a predefined altitude range, thus $z_i \in [z_i^{\min}, z_i^{\max}], i \in I_n$ with $z_i^{\min} \leq z_i^{\max}$. These altitude constraints ensure the safe operation of the MAA by avoiding collisions with ground obstacles as well as ensuring they remain within communication range of their base stations.

In addition, each MAA comes equipped with an onboard visual sensor capable of pan and tilt movements. Moreover, the sensor has a conical field of view and is able to alter its zoom. We denote the sensor's pan and tilt angles h_i and θ_i respectively, while its zoom level is represented by the angle of of the cone of vision which is denoted $2\delta_i$ with $\delta_i \in [\delta_i^{\min}, \delta_i^{\max}]$ and $\delta_i^{\min} \leq \delta_i^{\max} < \frac{\pi}{2}$.

Given the conical field of view of the sensors, its intersection with the plane will be a conic section which we call the sensing pattern. The sensing pattern is the region of the plane an MAA is able to cover. More specifically, it is a circle for $h_i = 0$, an ellipse for $0 < |h_i| < \frac{\pi}{2} - \delta_i$, a parabola for $\frac{\pi}{2} - \delta_i \leq |h_i| \leq \frac{\pi}{2} + \delta_i$ and a hyperbola for $\frac{\pi}{2} + \delta_i < |h_i|$. In the sequel we will examine only the case where $|h_i| < \frac{\pi}{2} - \delta_i$, i.e. circular and elliptical sensing patterns, in order to always have the sensing pattern bounded by a curve. In order to have static boundaries for the tilt angle we will constrain it inside the interval $(-h_i^{\max}, h_i^{\max}) \subseteq (-\frac{\pi}{2} + \delta_i, \frac{\pi}{2} - \delta_i)$ where $h_i^{\max} = \frac{\pi}{2} - \delta_i^{\max}$.

We define the center of the sensing footprint $q_{c,i} \in \Omega$ and denote the semi-major and semi minor axis of the elliptical sensing pattern a_i and b_i respectively. The unit vector $w_i \in \mathbb{R}^2$ indicates the orientation of the sensing pattern and is parallel to the semi-major axis of the ellipse if the sensing pattern is elliptical. These result in each MAA's sensing pattern being

$$C_i^s(X_i, h_i, \theta_i, \delta_i) = \mathbf{R}(\theta_i) C_i^b + q_{i,c}, \quad i \in I_n, \quad (1)$$

where \mathbf{R} is the 2×2 rotation matrix, $\|\cdot\|$ is the Euclidean metric and

$$C_i^b = \left\{ q \in \mathbb{R}^2 : \left\| \begin{bmatrix} \frac{1}{a_i} & 0 \\ 0 & \frac{1}{b_i} \end{bmatrix} q \right\| \leq 1 \right\}, \quad (2)$$

$$a_i = \frac{z_i}{2} [\tan(h_i + \delta_i) - \tan(h_i - \delta_i)], \quad (3)$$

$$b_i = z_i \tan(\delta_i) \sqrt{1 + \left[\frac{\tan(h_i + \delta_i) + \tan(h_i - \delta_i)}{2} \right]^2}, \quad (4)$$

$$q_{i,c} = q_i + w_i \frac{z_i}{2} [\tan(h_i + \delta_i) + \tan(h_i - \delta_i)], \quad (5)$$

$$w_i = [\cos(\theta_i) \quad \sin(\theta_i)]^T. \quad (6)$$

The pan angle θ_i only affects the sensing pattern's orientation, while the tilt angle h_i affects the eccentricity of the elliptical sensing pattern. It can be shown that if $h_i = 0$ then $a_i = b_i$ and C_i^s degenerates into a circle with $q_{c,i} = q_i$.

For the sake of simplicity, instead of using a complete dynamic model for the MAAs such as quadrotor dynamics, a single integrator kinematic model is used instead. The MAAs are approximated by point masses able to move in \mathbb{R}^3 . It is assumed that the visual sensors' pan and tilt angles and zoom can be controlled by onboard servos, thus their states are decoupled from those of the MAA. Therefore the kinematic model of each MAA is

$$\dot{q}_i = u_{i,q}, \quad q_i \in \Omega, \quad u_{i,q} \in \mathbb{R}^2, \quad (7)$$

$$\dot{z}_i = u_{i,z}, \quad z_i \in [z_i^{\min}, z_i^{\max}], \quad u_{i,z} \in \mathbb{R}, \quad (8)$$

$$\dot{\theta}_i = u_{i,\theta}, \quad \theta_i \in \mathbb{R}, \quad u_{i,\theta} \in \mathbb{R}, \quad (9)$$

$$\dot{h}_i = u_{i,h}, \quad h_i \in (-h_i^{\max}, h_i^{\max}), \quad u_{i,h} \in \mathbb{R}, \quad (10)$$

$$\dot{\delta}_i = u_{i,\delta}, \quad \delta_i \in [\delta_i^{\min}, \delta_i^{\max}], \quad u_{i,\delta} \in \mathbb{R}. \quad (11)$$

The projection on the ground $q_i \in \Omega$ of each agents position is assumed to be known with a degree of uncertainty, whereas each MAA's altitude z_i , sensor pan angle θ_i , tilt angle h_i and

view angle δ_i are known with certainty. Given an upper bound r_i for the positioning uncertainty of each MAA, its footprint q_i may reside anywhere with a disk called the positioning uncertainty region. The positioning uncertainty region, denoted C_i^u , is defined as

$$C_i^u(q_i, r_i) = \{ q \in \Omega : \|q - q_i\| \leq r_i \}, \quad i \in I_n. \quad (12)$$

Given the positioning uncertainty of each MAA, we also define the guaranteed sensed region $C_i^{gs} \subseteq C_i^s \subseteq \mathbb{R}^2$ as the region the MAA is guaranteed to cover for all its possible positions within C_i^u . The guaranteed sensed region is then defined as

$$C_i^{gs}(X_i, h_i, \theta_i, \delta_i, r_i) \triangleq \left\{ \bigcap_{q_i \in C_i^u} C_i^s \right\} \\ = \mathbf{R}(\theta_i) C_i^{bgs} + q_{i,c}, \quad i \in I_n, \quad (13)$$

where

$$C_i^{bgs} = \left\{ q \in \Omega : \left\| \begin{bmatrix} \frac{1}{a_i - r_i} & 0 \\ 0 & \frac{1}{b_i - r_i} \end{bmatrix} q \right\| \leq 1 \right\}. \quad (14)$$

Since the positioning uncertainty region C_i^u and sensed region C_i^s are circular and elliptical respectively, the guaranteed sensed region C_i^{gs} is also an ellipse. If C_i^s is a disk due to the tilt angle h_i being 0 then C_i^{gs} will also be a disk. If $r_i = 0$, i.e. the position of the MAA's footprint is known precisely, then $C_i^{gs} = C_i^s$. As $r_i \rightarrow \min(a_i, b_i)$ then C_i^{gs} approaches a line segment. For $r_i > \min(a_i, b_i)$ we get that $C_i^{gs} = \emptyset$. Figure 1 illustrates the visual coverage concept described in this section. The agent's guaranteed sensing pattern is shown filled in red for both $h_i = 0$ and $h_i \in (0, \frac{\pi}{2} - \delta_i)$.

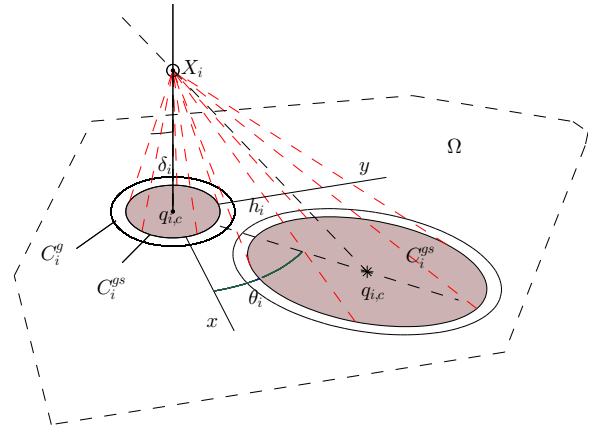


Fig. 1: Visual coverage concept.

Due to the nature of visual sensors, objects further away from the sensor appear with lower quality than ones near the sensor. We model the coverage quality using a quality function $f_i: [z_i^{\min}, +\infty) \rightarrow [0, 1]$, with 0 and 1 corresponding to the lowest and the highest possible quality respectively. In order to keep the control scheme simple, it is assumed that the coverage quality is uniform throughout each MAA's

sensed pattern. As the MAA's altitude z_i increases, the visual coverage quality of its sensed region decreases. The same is true while the sensor's tilt angle h_i increases, resulting in the center $q_{i,c}$ of the sensed pattern C_i^{gs} moving further away from the MAA. Similarly, zooming out, i.e. increasing δ_i , also leads in a decrease in quality. However, the sensor's pan angle θ_i as well as the agent's footprint q_i have no effect on the coverage quality. Except from being a decreasing function of z_i , h_i and δ_i , f_i must also be first-order differentiable with respect to z_i , h_i and δ_i within C_i^{gs} . This property is needed for computing the control law and will become apparent in the sequel.

Although any function having the previously mentioned properties could be chosen as the coverage quality function f_i , the following one was chosen arbitrarily

$$f_i(z_i, h_i, \delta_i) = \begin{cases} \frac{p(z_i, z_i^{\min}, z_i^{\max})}{3} + \frac{p(h_i, 0, h_i^{\max})}{3} \\ + \frac{p(\delta_i, \delta_i^{\min}, \delta_i^{\max})}{3}, & q \in C_i^{gs}, \\ 0, & q \notin C_i^{gs} \end{cases} \quad (15)$$

where

$$p(x, x^{\min}, x^{\max}) = \frac{\left((x - x^{\min})^2 - (x^{\max} - x^{\min})^2\right)^2}{(x^{\max} - x^{\min})^4}. \quad (16)$$

For the function p it holds that $p(x^{\min}, x^{\min}, x^{\max}) = 1$ and that $p(x^{\max}, x^{\min}, x^{\max}) = 0$. Consequently $f_i(z_i^{\min}, 0, \delta_i^{\min}) = 1$ and $\lim_{h_i \rightarrow h_i^{\max}} f_i(z_i^{\max}, h_i, \delta_i^{\max}) = 0$. The function f_i is also dependent on the agent's altitude, tilt and zoom constraints. It should be noted that this choice of quality function is not unique and that different quality functions result in different quality-coverage trade-offs.

Additionally, each point $q \in \Omega$ can be assigned an importance weight through a space density function $\phi: \Omega \rightarrow \mathbb{R}_+$ which expresses the a priori information regarding the importance of certain regions of Ω . We define the following joint coverage-quality objective

$$\mathcal{H} \triangleq \int_{\Omega} \max_{i \in I_n} f_i(z_i, h_i, \delta_i) \phi(q) dq. \quad (17)$$

This function accounts for both the area covered by the agents and the coverage quality over that area, while also taking into account the importance of points as encoded by $\phi(q)$. The goal of the MAA team is to maximize this objective. To that extent, a suitable partitioning scheme will be employed in order to distribute the computation of \mathcal{H} among the agents. Then a gradient-based control law will be designed to lead the MAA team to a locally optimal configuration with respect to \mathcal{H} .

III. AREA PARTITIONING STRATEGY

The most common choice of partitioning scheme for area coverage problems is the Voronoi diagram and similar diagrams inspired by it. Voronoi-like diagrams that can take into account the positioning uncertainty of mobile agents have been proposed in the past [18], [19]. However in this work a partitioning of just the sensed space is utilized, similarly to [22]. This partitioning scheme assigns a region of responsibility (cell) to each agent based on guaranteed sensed regions C_i^{gs}

and the coverage quality over them. Each MAA is assigned a cell W_i as follows

$$W_i \triangleq \{q \in \Omega: f_i > f_j, i \neq j\}, i \in I_n. \quad (18)$$

However the union these cells does not comprise a complete tessellation of the total guaranteed sensed region $\bigcup_{i \in I_n} C_i^{gs}$. This is due to the fact that regions sensed by multiple agents with the same coverage quality are left unassigned. These so called common regions still contribute towards the objective \mathcal{H} so they must be taken into account. The set of agents with the same coverage quality f^l and overlapping guaranteed sensed regions is

$$\mathcal{I}_l = \left\{ i, j \in I_n, i \neq j: C_i^{gs} \cap C_j^{gs} \neq \emptyset \right. \\ \left. \wedge f_i = f_j = f^l \right\}, l \in I_L.$$

The common regions are then computed as

$$W_c^l = \left\{ \exists i, j \in \mathcal{I}_l, i \neq j: q \in C_i^{gs} \cap C_j^{gs} \right\}, l \in I_L. \quad (19)$$

By utilizing the partitioning strategy (18), (19), coverage-quality objective (17) can be written as

$$\mathcal{H} = \sum_{i \in I_n} \int_{W_i} f_i \phi(q) dq + \sum_{l=1}^L \int_{W_c^l} f^l \phi(q) dq \quad (20)$$

Remark 1: We define the neighbors N_i of an agent i as

$$N_i \triangleq \left\{ j \in I_n \setminus i: C_i^{gs} \cap C_j^{gs} \neq \emptyset \right\}. \quad (21)$$

The neighbors of an agent i are essentially the agents that affect the cell W_i of agent i , thus they are the agents i must be able to exchange information with.

By allowing the MAAs' cameras to tilt it is possible that the sensed regions of two distant MAAs overlap. Since the partitioning scheme is based on the sensed regions, these MAAs should be able to communicate. However this might not always be practical given their distance. An algorithm for propagating state information in a mobile agent network has been proposed in [21]. By utilizing this algorithm MAAs are able to exchange information with their neighbors in multiple hops instead of communicating directly.

Remark 2: Since the partitioning scheme (18), (19) only partitions the guaranteed sensed region $\bigcup_{i \in I_n} C_i^{gs}$, a portion of Ω is left unpartitioned. This region is called the neutral region, is denoted \mathcal{O} and can be computed as

$$\mathcal{O} = \Omega \setminus \left\{ \bigcup_{i \in I_n} W_i \cup \bigcup_{l \in I_L} W_c^l \right\} = \Omega \setminus \bigcup_{i \in I_n} C_i^{gs}. \quad (22)$$

Remark 3: Due to the fact that the coverage quality f_i is constant throughout the guaranteed sensed region C_i^{gs} , the resulting cells W_i are bounded by elliptical arcs of C_i^{gs} . Moreover, this partitioning scheme may result in some cells being non-convex, empty or consisting of multiple disjoint regions. However all of these cases are handled properly by the designed control law without the need for extensions.

IV. COLLABORATIVE CONTROL DEVELOPMENT

Having defined the partitioning scheme (18), (19) which allows distributing the computation of the objective \mathcal{H} among the agents, what remains is the derivation of the gradient-based control law.

Theorem 1: Given a team of MAAs with kinematics described by (7), (8), (9), (10), (11), sensing performance (1) and positioning uncertainty (12), the following control law guarantees monotonic increase of the coverage-quality objective (20) along the MAAs trajectories.

$$u_{i,q} = K_{i,q} \left[\int_{\partial W_i \cap \partial \mathcal{O}} u_i^i n_i f_i \phi(q) dq + \sum_{j \in I_n, j \neq i} \int_{\partial W_i \cap \partial W_j} u_i^i n_i (f_i - f_j) \phi(q) dq \right], \quad (23)$$

$$u_{i,z} = K_{i,z} \left[\int_{\partial W_i \cap \partial \mathcal{O}} v_i^i n_i f_i \phi(q) dq + \int_{W_i} \frac{\partial f_i}{\partial z_i} \phi(q) dq + \sum_{j \in I_n, j \neq i} \int_{\partial W_i \cap \partial W_j} v_i^i n_i (f_i - f_j) \phi(q) dq \right], \quad (24)$$

$$u_{i,\theta} = K_{i,\theta} \left[\int_{\partial W_i \cap \partial \mathcal{O}} \tau_i^i n_i f_i \phi(q) dq + \sum_{j \in I_n, j \neq i} \int_{\partial W_i \cap \partial W_j} \tau_i^i n_i (f_i - f_j) \phi(q) dq \right], \quad (25)$$

$$u_{i,h} = K_{i,h} \left[\int_{\partial W_i \cap \partial \mathcal{O}} \sigma_i^i n_i f_i \phi(q) dq + \int_{W_i} \frac{\partial f_i}{\partial h_i} \phi(q) dq + \sum_{j \in I_n, j \neq i} \int_{\partial W_i \cap \partial W_j} \sigma_i^i n_i (f_i - f_j) \phi(q) dq \right], \quad (26)$$

$$u_{i,\delta} = K_{i,\delta} \left[\int_{\partial W_i \cap \partial \mathcal{O}} \mu_i^i n_i f_i \phi(q) dq + \int_{W_i} \frac{\partial f_i}{\partial \delta_i} \phi(q) dq + \sum_{j \in I_n, j \neq i} \int_{\partial W_i \cap \partial W_j} \mu_i^i n_i (f_i - f_j) \phi(q) dq \right], \quad (27)$$

where $K_{i,q}, K_{i,z}, K_{i,\theta}, K_{i,h}, K_{i,\delta}$ are positive constants, n_i the outward pointing unit normal vector on W_i and $u_i^i, v_i^i, \tau_i^i, \sigma_i^i, \mu_i^i$ the Jacobian matrices

$$u_j^i \triangleq \frac{\partial q}{\partial q_i}, \quad q \in \partial W_j, i, j \in I_n \quad (28)$$

$$v_j^i \triangleq \frac{\partial q}{\partial z_i}, \quad q \in \partial W_j, i, j \in I_n \quad (29)$$

$$\tau_j^i \triangleq \frac{\partial q}{\partial \theta_i}, \quad q \in \partial W_j, i, j \in I_n \quad (30)$$

$$\sigma_j^i \triangleq \frac{\partial q}{\partial h_i}, \quad q \in \partial W_j, i, j \in I_n \quad (31)$$

$$\mu_j^i \triangleq \frac{\partial q}{\partial \delta_i}, \quad q \in \partial W_j, i, j \in I_n \quad (32)$$

Proof: In order to guarantee monotonic increase of \mathcal{H} , its time derivative is evaluated as

$$\frac{\partial \mathcal{H}}{\partial t} = \frac{\partial \mathcal{H}}{\partial q_i} \dot{q}_i + \frac{\partial \mathcal{H}}{\partial z_i} \dot{z}_i + \frac{\partial \mathcal{H}}{\partial \theta_i} \dot{\theta}_i + \frac{\partial \mathcal{H}}{\partial h_i} \dot{h}_i + \frac{\partial \mathcal{H}}{\partial \delta_i} \dot{\delta}_i \quad (33)$$

By selecting the following control inputs

$$u_{i,q} = K_{i,q} \frac{\partial \mathcal{H}}{\partial q_i}, u_{i,z} = K_{i,z} \frac{\partial \mathcal{H}}{\partial z_i}, \\ u_{i,\theta} = K_{i,\theta} \frac{\partial \mathcal{H}}{\partial \theta_i}, u_{i,h} = K_{i,h} \frac{\partial \mathcal{H}}{\partial h_i}, u_{i,\delta} = K_{i,\delta} \frac{\partial \mathcal{H}}{\partial \delta_i},$$

we guarantee, given the MAAs dynamics, that $\frac{\partial \mathcal{H}}{\partial t}$ is non-negative since

$$\frac{\partial \mathcal{H}}{\partial t} = \left[K_{i,q} \left(\frac{\partial \mathcal{H}}{\partial q_i} \right)^2 + K_{i,z} \left(\frac{\partial \mathcal{H}}{\partial z_i} \right)^2 + K_{i,\theta} \left(\frac{\partial \mathcal{H}}{\partial \theta_i} \right)^2 + K_{i,h} \left(\frac{\partial \mathcal{H}}{\partial h_i} \right)^2 + K_{i,\delta} \left(\frac{\partial \mathcal{H}}{\partial \delta_i} \right)^2 \right] \geq 0,$$

where $K_{i,q}, K_{i,z}, K_{i,\theta}, K_{i,h}, K_{i,\delta}$ are positive constants, thus, ensuring that the coverage-quality criterion increases in a monotonic manner.

The partial derivative $\frac{\partial \mathcal{H}}{\partial q_i}$ is

$$\frac{\partial \mathcal{H}}{\partial q_i} = \frac{\partial}{\partial q_i} \left\{ \sum_{i \in I_n} \int_{W_i} f_i \phi(q) dq + \sum_{l=1}^L \int_{W_c^l} f^l \phi(q) dq \right\}.$$

By applying the Leibniz integral rule and since $\frac{\partial f_i(z_i, h_i, \delta_i)}{\partial q_i} = \frac{\partial f_j(z_j, h_j, \delta_j)}{\partial q_i} = 0$ the previous equation yields

$$\frac{\partial \mathcal{H}}{\partial q_i} = \int_{\partial W_i} u_i^i n_i f_i \phi(q) dq + \sum_{j \in I_n, j \neq i} \int_{\partial W_i \cap \partial W_j} u_j^i n_j f_j \phi(q) dq.$$

We use a boundary decomposition of ∂W_i into disjoint sets similarly to [22]

$$\partial W_i = \left\{ \{ \partial W_i \cap \partial \Omega \} \cup \{ \partial W_i \cap \partial \mathcal{O} \} \cap \left\{ \bigcup_{i \neq j} \partial W_i \cap \partial W_j \right\} \cap \left\{ \bigcup_{l=1}^L \partial W_i \cap \partial W_c^l \right\} \right\} \quad (34)$$

and assuming a static region of interest Ω . In addition, since $\partial W_i \cup \partial W_c^l$ are subsets of some sensed region boundary ∂C_j , independent of the state of node i , at $q \in \left\{ \partial \Omega \cap \partial W_i \right\}$ and $q \in \left\{ \partial W_i \cup \partial W_c^l \right\}$, the Jacobian matrix is $u_i^i = \mathbf{0}_{2 \times 2}$ resulting

in the final expression for $\frac{\partial \mathcal{H}}{\partial q_i}$

$$\frac{\partial \mathcal{H}}{\partial q_i} = \int_{\partial W_i \cap \partial \mathcal{O}} u_i^i n_i f_i \phi(q) dq + \sum_{j \in I_n, j \neq i} \int_{\partial W_i \cap \partial W_j} u_j^i n_i [f_i - f_j] \phi(q) dq.$$

Through a similar procedure and given that $\frac{\partial f_j}{\partial z_i} = \frac{\partial f_j}{\partial \theta_i} = \frac{\partial f_j}{\partial h_i} = \frac{\partial f_j}{\partial \delta_i} = 0$ we obtain the rest of the control laws. ■

V. SIMULATION STUDIES

Simulation studies were conducted in order to evaluate the efficiency of the proposed control strategy. For consistency, the region of interest Ω was selected to be the same as in [19]. The space density function was assumed to be $\phi(q) = 1, \forall q \in \Omega$, assigning equal importance to all points inside the region of interest. The camera state limits were $h_i^{\max} = 50^\circ$, $\delta_i^{\min} = 15^\circ$ and $\delta_i^{\max} = 35^\circ$, $\forall i \in I_n$. The MAAs cells are shown filled in grey with solid black boundaries while the boundaries of guaranteed sensed regions are shown in dashed red lines in Figures 2 (a) and (b) and Figures 4 (a) and (b). The MAAs' trajectories are shown as blue lines Figures 2 (b) and 4 (b).

A. Case study I

This simulation examines the case of a team of 3 MAAs and it serves to highlight the fact that there exists a configuration with respect to the agents' altitude z_i , camera tilt angle h_i and zoom δ_i that is globally optimal. The MAAs altitude constraints were set to $z_i^{\min} = 0.3$ and $z_i^{\max} = 3.8 \forall i \in I_3$. The initial and final configurations of the swarm are shown in Figures 2 (a) and 2 (b) respectively. We observe from Figure 2 (b) that the MAAs guaranteed sensed regions do not overlap and are completely contained inside Ω . This indicates that the MAA team has reached a globally optimal configuration. It should be noted that due to the fact that no closed-form expression exists for the arc length of an ellipse, it is impossible to analytically compute the altitude, tilt angle and zoom that result in this configuration. This simulation study was also conducted with agents equipped with downward facing cameras unable to pan, tilt or zoom as in [20]. Figure 3 shows the evolution of the coverage-quality objective \mathcal{H} over time for both the pan-tilt-zoom and downwards facing cameras in solid black and dashed red respectively. It is observed that by allowing the MAAs' cameras to pan, tilt and zoom, it is possible to achieve significantly higher coverage performance. Finally, it is observed that the monotonic increase of \mathcal{H} has been achieved, confirming that the control design and implementation is correct.

B. Case study II

A team of 6 MAAs is simulated in this case study. The MAAs altitude constraints were set to $z_i^{\min} = 0.3$ and $z_i^{\max} = 1.8 \forall i \in I_6$. The initial and final configurations of the MAA team are shown in Figures 4 (a) and 4 (b) respectively. Due to the greater number of agents in this simulation there is overlapping between their guaranteed sensed regions and the MAA team has not reached a globally optimal configuration with respect to \mathcal{H} . However the MAAs do reach a locally optimal configuration as was expected. This simulation study was also repeated with cameras unable to pan, tilt and zoom. Figure 5 shows the evolution of the coverage-quality objective \mathcal{H} over time for both the pan-tilt-zoom and downwards facing cameras in solid black and dashed red respectively. Once again the benefits of using pan-tilt-zoom cameras become apparent and it is once again observed that \mathcal{H} does indeed increase monotonically.

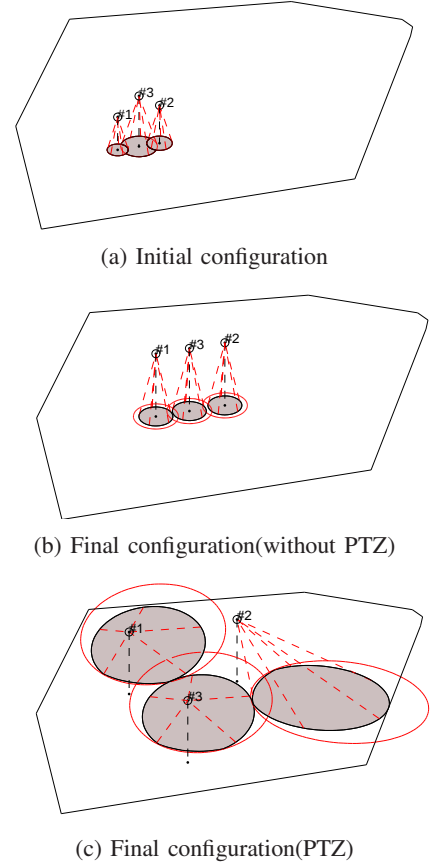


Fig. 2: Simulation I

VI. CONCLUSIONS

In this article, the efficiency collaborative visual aerial coverage by a swarm of MAAs, equipped with cameras able to pan, tilt and zoom while operating under positional uncertainty, has been examined. Regarding the partitioning, a Voronoi-free strategy has been utilized upon which a gradient-based control law was derived guaranteeing monotonic increase of the coverage quality criterion. Simulation studies

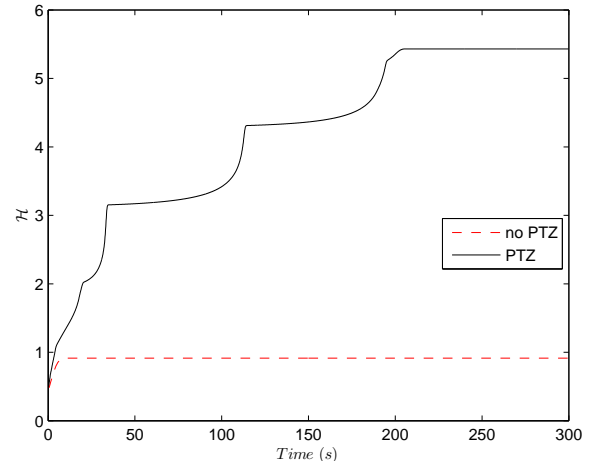


Fig. 3: Case study I: Coverage-quality objective evolution.

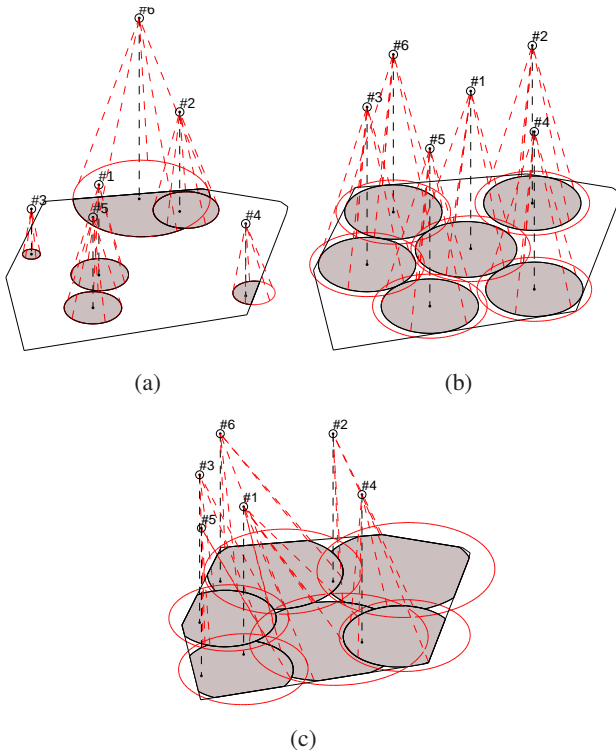


Fig. 4: Simulation II: Initial (a) and final configurations without PTZ-cameras (b) and with PTZ-cameras (c).

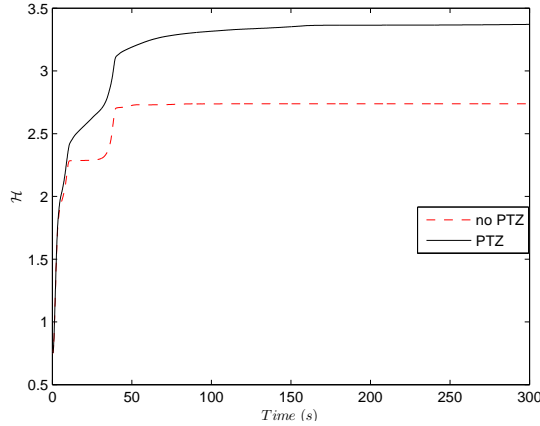


Fig. 5: Simulation II: Coverage-quality objective.

were offered to evaluate the efficiency of the PTZ extended configuration in contrast with the downwards, not zoom-enabled cameras.

REFERENCES

- [1] F. Abbasi, A. Mesbahi, and J. M. Velni, "A team-based approach for coverage control of moving sensor networks," *Automatica*, vol. 81, pp. 342–349, 2017.
- [2] A. Pierson, L. C. Figueiredo, L. C. A. Pimenta, and M. Schwager, "Adapting to sensing and actuation variations in multi-robot coverage," *The International Journal of Robotics Research*, vol. 36, no. 3, pp. 337–354, 2017.
- [3] J. M. Palacios-Gasós, E. Montijano, C. Sagüés, and S. Llorente, "Distributed coverage estimation and control for multirobot persistent tasks," *IEEE Transactions on Robotics*, vol. PP, no. 99, pp. 1–17, 2016.
- [4] C. Franco, D. M. Stipanović, G. López-Nicolás, C. Sagüés, and S. Llorente, "Persistent coverage control for a team of agents with collision avoidance," *European Journal of Control*, vol. 22, pp. 30–45, 2015.
- [5] Y. Kantaros, M. Thanou, and A. Tzes, "Distributed coverage control for concave areas by a heterogeneous robot-swarm with visibility sensing constraints," *Automatica*, vol. 53, pp. 195–207, 2015.
- [6] R. J. Alitappeh, K. Jeddissaravi, and F. G. Guimarães, "Multi-objective multi-robot deployment in a dynamic environment," *Soft Computing*, vol. 21, no. 21, pp. 1–17, 2016.
- [7] F. Sharifi, A. Chamseddine, H. Mahboubi, Y. Zhang, and A. G. Aghdam, "A distributed deployment strategy for a network of cooperative autonomous vehicles," *IEEE Transactions on Control Systems Technology*, vol. 23, no. 2, pp. 737–745, 2015.
- [8] J. M. Luna, R. Fierro, C. Abdallah, and J. Wood, "An adaptive coverage control algorithm for deployment of nonholonomic mobile sensors," in *Proceedings 49th IEEE Conference on Decision and Control (CDC)*, Dec. 2010, pp. 1250–1256.
- [9] Y. Stergiopoulos and A. Tzes, "Cooperative positioning/orientation control of mobile heterogeneous anisotropic sensor networks for area coverage," in *Proceedings IEEE International Conference on Robotics and Automation (ICRA)*, Hong Kong, China, 2014, pp. 1106–1111.
- [10] O. Arslan and D. E. Koditschek, "Voronoi-based coverage control of heterogeneous disk-shaped robots," in *2016 IEEE International Conference on Robotics and Automation (ICRA)*. Stockholm, Sweden: IEEE, 2016, pp. 4259–4266.
- [11] Y. Stergiopoulos, M. Thanou, and A. Tzes, "Distributed collaborative coverage-control schemes for non-convex domains," *IEEE Transactions on Automatic Control*, vol. 60, no. 9, pp. 2422–2427, 2015.
- [12] C. Nowzari and J. Cortés, "Self-triggered coordination of robotic networks for optimal deployment," *Automatica*, vol. 48, no. 6, pp. 1077–1087, 2012.
- [13] V. Ramaswamy and J. R. Marden, "A sensor coverage game with improved efficiency guarantees," in *Proceedings American Control Conference (ACC)*, Boston, MA, USA, July 2016, pp. 6399–6404.
- [14] A. Kwok and S. Martinez, "A distributed deterministic annealing algorithm for limited-range sensor coverage," *IEEE Transactions on Control Systems Technology*, vol. 19, no. 4, pp. 792–804, 2011.
- [15] A. Mavrommati, E. Tzorakoleftherakis, I. Abraham, and T. D. Murphey, "Real-time area coverage and target localization using receding-horizon ergodic exploration," *IEEE Transactions on Robotics*, vol. 34, no. 1, pp. 62–80, 2018.
- [16] J. Habibi, H. Mahboubi, and A. G. Aghdam, "Distributed coverage control of mobile sensor networks subject to measurement error," *IEEE Transactions on Automatic Control*, vol. 61, no. 11, pp. 3330–3343, Nov. 2016.
- [17] B. Davis, I. Karamouzas, and S. J. Guy, "C-OPT: Coverage-aware trajectory optimization under uncertainty," *IEEE Robotics and Automation Letters*, vol. 1, no. 2, pp. 1020–1027, July 2016.
- [18] S. Papatheodorou, A. Tzes, K. Giannousakis, and Y. Stergiopoulos, "Distributed area coverage control with imprecise robot localization: Simulation and experimental studies," *International Journal of Advanced Robotic Systems*, vol. 15, no. 5, Sept. 2018.
- [19] M. Tzes, S. Papatheodorou, and A. Tzes, "Visual area coverage by heterogeneous aerial agents under imprecise localization," *IEEE Control Systems Letters*, vol. 2, no. 4, pp. 623–628, Oct. 2018.
- [20] S. Papatheodorou, A. Tzes, and Y. Stergiopoulos, "Collaborative visual area coverage," *Robotics and Autonomous Systems*, vol. 92, pp. 126–138, June 2017.
- [21] M. Schwager, B. J. Julian, M. Angermann, and D. Rus, "Eyes in the sky: Decentralized control for the deployment of robotic camera networks," *Proceedings of the IEEE*, vol. 99, no. 9, pp. 1541–1561, 2011.
- [22] S. Papatheodorou and A. Tzes, "Cooperative visual convex area coverage using a tessellation-free strategy," in *56th IEEE Conference on Decision and Control (CDC)*, Melbourne, Australia, Dec. 2017, pp. 4662–4667.
- [23] O. Arslan, H. Min, and D. E. Koditschek, "Voronoi-based coverage control of pan/tilt/zoom camera networks," in *Robotics and Automation (ICRA)*, 2018 IEEE International Conference on. IEEE, 2018.
- [24] N. Bousias, S. Papatheodorou, M. Tzes, and A. Tzes, "Collaborative visual area coverage using aerial agents equipped with ptz-cameras under localization uncertainty," in *2019 18th European Control Conference (ECC)*, June 2019, pp. 1079–1084.